Scattering of light from small nematic spheres with radial dielectric anisotropy

Huseyin Karacali,[1] Steven M. Risser,[1] and Kim F. Ferris[2]
[1]*Department of Physics, Texas A&M University–Commerce, Commerce, Texas 75429*
[2]*Department of Materials Sciences, Pacific Northwest National Laboratories, Richland, Washington 99352*
(Received 5 May 1997)

We have calculated the scattering cross sections of small anisotropic nematic droplets embedded in a polymer matrix as a function of the dielectric constants of the nematic and the polymer. We have derived the general form for the Helmholtz wave equation for a droplet which has spatially varying radial anisotropy, and have explicitly solved this equation for three distinct models of the dielectric anisotropy, including one model where the anisotropy increases linearly with droplet radius. Numerical calculations of the scattering amplitudes for droplets much smaller than the wavelength of the incident radiation show that droplets with continual variation in the dielectric anisotropy have much larger scattering amplitude than droplets with fixed anisotropy. The scattering from droplets with linearly varying anisotropy exhibits a scattering minimum for much smaller polymer dielectric constants than the other models. These results show that the scattering from small anisotropic droplets is sensitive to details of the internal structure and anisotropy of the droplet.
[S1063-651X(97)04810-1]

PACS number(s): 61.30.−v, 42.70.Df

I. INTRODUCTION

There has been much recent interest in scattering from anisotropic spheres. In the field of liquid crystals, this interest has been stimulated by the development of a new generation of displays and electro-optical devices [1] based on polymer dispersed liquid crystals [2–7] (PDLC's). These materials consist of dispersions of small liquid crystal droplets embedded in a uniform polymer matrix. The optical properties of PDLC's are controlled by modulating the structure of the nematic director with an external electric field. Variation of the director alters the effective index of refraction of the droplet, changing the transparency of the PDLC [8].

The droplet structure and its optical properties are determined from the positional dependence of the nematic order parameter, which is a second rank tensor. However, the only required quantities for uniaxial nematics are the director field [9,10] and the positional dependence of the scalar order parameter S, which describes the degree of alignment of molecules with the director. The director configuration is dependent on many factors, including the size of the droplet, elastic constants of the nematic, the anchoring energy, the orientation at the nematic-polymer interface, and the magnitude of an external electric or magnetic field [11–13]. For droplets with strong normal anchoring and no external field [12,14,15], a commonly observed director configuration is the radial configuration, where the director is oriented along the radial unit vector. The dielectric tensor for a droplet with a radial director configuration is diagonal in spherical coordinates, with a value ε_r in the radial direction and ε_t in the tangential directions. The magnitude of the components, and the anisotropy, is determined by the magnitude of the order parameter (S) in the nematic phase [16]

$$\varepsilon_r = \varepsilon_{\rm iso} + \tfrac{2}{3}\varepsilon_a S, \quad \varepsilon_t = \varepsilon_{\rm iso} - \tfrac{1}{3}\varepsilon_a S, \tag{1}$$

where $\varepsilon_{\rm iso}$ is the dielectric constant for the isotropic phase, and ε_a is the maximum dielectric anisotropy. S ranges from 0 in the isotropic phase to 1 in the perfectly ordered phase.

There have been several previous scattering studies of droplets with radial anisotropy. Roth and Dignam [17] derived the general form (series expansion) for the scattering cross section for spheres with constant radial anisotropy, and explicitly calculated the cross section as a function of droplet parameters in the small particle limit. Aragon and Pecora [18] and Lange and Aragon [19] determined a closed-form solution for scattering from a thin radially anisotropic layer on an isotropic sphere. Zumer and Doane [20–22] calculated the scattering cross section for radial directors within the Rayleigh-Gans approximation. However, these previous studies have limited applicability to small nematic droplets because they assumed an outer region of constant anisotropy (order parameter) with an isotropic central region. Recent work [23] has shown that while large ($R \geqslant 0.22$ mm) nematic droplets satisfy this condition, smaller droplets have anisotropy that varies continually throughout the droplet.

In this work, we will calculate the scattering from small nematic droplets in the spherically symmetric (zero external field) radial director configuration. To determine how spatially varying anisotropy alters the scattering, we will perform calculations for three distinct models of the anisotropy. The central defect model (Fig. 1) assumes a small isotropic defect at the center of the droplet, and constant order parameter at all points exterior to the defect and still inside the droplet. This is the model that was used in the previous studies [17–22]. The second model is the linear defect model, where the order parameter increases linearly within a small central defect region, and is constant throughout the remainder of the droplet. This model is representative of droplets with strong anchoring at the nematic-polymer interface [23]. Small droplets with weak surface anchoring do not have any region where the order parameter is constant. To illustrate the role of continually varying order parameter, we use the linear model, in which the order parameter varies linearly with distance from the droplet origin. The results from this

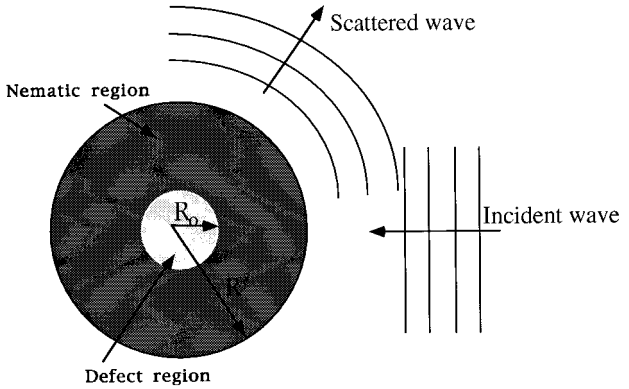

FIG. 1. Defect model of a droplet. The region between R_0 and R has constant radial anisotropy and dielectric components ε_r and ε_t. In the central defect model, the region inside R_0 is isotropic with dielectric constant ε_1. In the linear defect model, the dielectric anisotropy grows linearly from zero at the origin to the anisotropy of the nematic phase at the boundary. The region exterior to the droplet has dielectric constant ε_3.

simple model with spherically symmetric dielectric anisotropy illustrate that scattering calculations for nematic droplets must include details of the internal structure.

In the following, we derive the wave equation for a medium with spatially varying, but spherically symmetric, dielectric anisotropy. From the boundary conditions on the fields at the droplet surface, we determine the scattering amplitude as a function of the dielectric properties of the droplet and the surrounding medium. We develop the explicit solution for the linear model and the linear defect model in the small-particle limit. We then compare scattering amplitudes from these models to those from the central defect model, which has been used previously in studies on small nematic droplets. Finally, we discuss these results, draw conclusions, and present possible extensions of this work.

II. WAVE EQUATION IN AN ANISOTROPIC MEDIUM

For a harmonic electromagnetic wave, the time-independent parts of the electric and magnetic vectors in all three media satisfy

$$\nabla\times\mathbf{H}=\frac{i\omega}{c}\,\varepsilon\mathbf{E}, \tag{2a}$$

$$\nabla\times\mathbf{E}=-\frac{i\omega}{c}\,\mathbf{H}. \tag{2b}$$

Writing Eq. (2a) explicitly in spherical coordinates gives

$$\frac{1}{r^2\sin\theta}\left(\frac{\partial(rH_\phi\sin\theta)}{\partial\theta}-\frac{\partial(rH_\theta)}{\partial\phi}\right)=\frac{i\omega}{c}\,\varepsilon_r E_r, \tag{3a}$$

$$\frac{1}{r\sin\theta}\left(\frac{\partial H_r}{\partial\phi}-\frac{\partial(rH_\phi\sin\theta)}{\partial r}\right)=\frac{i\omega}{c}\,\varepsilon_t E_\theta, \tag{3b}$$

$$\frac{1}{r}\left(\frac{\partial(rH_\theta)}{\partial r}-\frac{\partial(H_r)}{\partial\theta}\right)=\frac{i\omega}{c}\,\varepsilon_t E_\phi. \tag{3c}$$

In any isotropic region, $\varepsilon_t=\varepsilon_r$. Equation (2b) leads to a similar set of equations, but not containing ε_t or ε_r.

We will represent the solution of these equations as a superposition of two linearly independent fields $({}^eH,{}^eH)$ and $({}^mE,{}^mH)$ each satisfying the conditions [24]

$${}^eE_r=E_r,\quad {}^eH_r=0$$

$${}^mE_r=0,\quad {}^mH_r=H.$$

The solution with vanishing radial magnetic field is called the electric wave (TM wave), and that with vanishing radial electric field is called the magnetic wave (TE wave). In the following, we will only discuss the electric wave. If the magnetization of each medium is isotropic, the solution for these waves is known [25,26] and has been discussed previously. If the magnetization is also anisotropic, the solutions will correspond to those derived in the following.

We now define the standard Debye potential for the electric wave from

$$E_\phi=\frac{1}{r\sin\theta}\frac{\partial}{\partial\phi}\left(\frac{\partial(r{}^e\Pi)}{\partial r}\right),\quad E_\theta=\frac{1}{r}\frac{\partial^2(r{}^e\Pi)}{\partial\theta\partial r},$$
$$H_\phi=\frac{k_t}{r}\frac{\partial(r{}^e\Pi)}{\partial\theta},\quad H_\theta=-\frac{k_t}{r\sin\theta}\frac{\partial(r{}^e\Pi)}{\partial\phi}, \tag{4}$$

where ${}^e\Pi$ is the Debye potential for the electric wave and $k_t=\omega\varepsilon_t/c$. From these definitions, it can be shown that the Debye potential must then obey

$$\frac{\varepsilon_r}{\varepsilon_t}\frac{1}{r}\frac{\partial^2(r{}^e\Pi)}{\partial r^2}+\frac{\varepsilon_r\varepsilon_t'}{\varepsilon_t^2 r}\frac{\partial(r{}^e\Pi)}{\partial r}+\frac{1}{r^2\sin\theta}\frac{\partial}{\partial\theta}\left(\sin\theta\,\frac{\partial{}^e\Pi}{\partial\theta}\right)$$
$$+\frac{1}{r^2\sin^2\theta}\frac{\partial^2\,{}^e\Pi}{\partial\phi^2}+\left(\frac{\omega^2\varepsilon_r}{c^2}-\frac{\varepsilon_r\varepsilon_t'^2}{\varepsilon_t^3}+\frac{\varepsilon_r\varepsilon_t''}{\varepsilon_t^2}\right)r{}^e\Pi=0, \tag{5}$$

where

$$\varepsilon_t'=\frac{d\varepsilon_t}{dr},\quad \varepsilon_t''=\frac{d^2\varepsilon_t}{dr^2}, \tag{6}$$

This is the Helmholtz wave equation, generalized to the case where the dielectric properties are a function of r. In the limit that ε_t is constant, Eq. (5) reduces to that reported previously [17]. In the limit that $\varepsilon_t=\varepsilon_r$, Eq. (5) reduces to the standard Helmholtz equation.

Equation (5) is separable, with the angular solution the standard spherical harmonics, $Y_L^m(\theta\phi)$. The differential equation for the radial function, $Q(r)$, is then given by

$$r^2\frac{\partial^2(rQ)}{\partial r^2}+r^2\frac{\varepsilon_t'}{\varepsilon_t}\frac{\partial(rQ)}{\partial r}+\left((k_t r)^2-\frac{\varepsilon_t'^2}{\varepsilon_t^2}r^2+\frac{\varepsilon_t''}{\varepsilon_t}r^2\right.$$
$$\left.-L(L+1)\frac{\varepsilon_t}{\varepsilon_r}\right)(rQ)=0. \tag{7}$$

To this point, the derivation has made no assumptions about the dielectric anisotropy, other than requiring it to be a function of r only. To proceed further with the calculations, we

must specify the functional form of the dielectric constants. In the following, we solve for three distinct models of the radial anisotropy.

III. SOLUTION OF THE ANISOTROPIC WAVE EQUATION

External isotropic medium

In the region exterior to the droplet, the material is optically isotropic (dielectric constant ε_3), so the radial equation reduces to

$$r^2\frac{\partial^2(rQ)}{\partial r^2}+((k_t r)^2-L(L+1))(rQ)=0. \tag{8}$$

The solutions of this equation are the standard spherical Bessel functions. The incident wave (of unit amplitude) is then represented as

$$r^e\Pi^{(i)}=\frac{1}{k_3^2}\sum_{L=1}^{\infty} i^{L-1}\frac{2L+1}{L(L+1)}(\pi k_3 r/2)^{1/2}J_{L+1/2}(k_3 r)\times P_L^{(1)}(\cos\theta)\cos\phi, \tag{9a}$$

$$r^m\Pi^{(i)}=\frac{1}{k_3^2}\sum_{L=1}^{\infty} i^{L-1}\frac{2L+1}{L(L+1)}(\pi k_3 r/2)^{1/2}J_{L+1/2}(k_3 r)\times P_L^{(1)}(\cos\theta)\sin\phi. \tag{9b}$$

For the scattered wave, Neumann functions can be used as the second solution since the scattered wave must vanish at infinity and the region of the interest does not contain the origin:

$$r^e\Pi^{(s)}=-\frac{1}{k_3^2}\sum_{L=1}^{\infty} i^{L-1}\frac{2L+1}{L(L+1)}(\pi k_3 r/2)^{1/2}a_L\{J_{L+1/2}(k_3 r)+iJ_{-L-1/2}(k_3 r)\}P_L^{(1)}(\cos\theta)\cos\phi, \tag{10a}$$

$$r^m\Pi^{(s)}=-\frac{1}{k_3^2}\sum_{L=1}^{\infty} i^{L-1}\frac{2L+1}{L(L+1)}\times(\pi k_3 r/2)^{1/2}b_L\{J_{L+1/2}(k_3 r)+iJ_{-L-1/2}(k_3 r)\}\times P_L^{(1)}(\cos\theta)\sin\phi. \tag{10b}$$

The scattering cross section is then given by

$$C_{\mathrm{sca}}=(\lambda^2/2\pi)\sum_{L=1}^{\infty}(2L+1)\{|a_L|^2+|b_L|^2\}, \tag{11}$$

where λ is the wavelength of the incident radiation.

Linear anisotropy region

In this region, we assume that both the radial and tangential components of the dielectric tensor vary linearly with radius, while keeping the trace of the dielectric tensor constant. The components of the tensor can be represented as

$$\varepsilon_r=\varepsilon_2+2\beta r,\quad \varepsilon_t=\varepsilon_2-\beta r,\quad \beta=\varepsilon_a/R. \tag{12}$$

The differential equation for the radial function becomes

$$\varepsilon_t^2\varepsilon_r r^2\frac{\partial^2(rQ)}{\partial r^2}-\beta\varepsilon_r\varepsilon_t r^2\frac{\partial(rQ)}{\partial r}+(\varepsilon_t^2\varepsilon_r(k_t r)^2-\beta^2\varepsilon_r r^2-L(L+1)\varepsilon_t^3)(rQ)=0. \tag{13}$$

If we assume rQ can be expanded in a power series

$$rQ=\sum_{n=0}A_n(k_t r)^{n+s}. \tag{14}$$

Gathering terms by powers of r gives

$$\begin{aligned}&\sum_{n=0}[\varepsilon_2^3(n+s)(n+s-1)-L(L+1)\varepsilon_2^3]A_n(k_t r)^{n+s}\\&+\sum_{n=0}[3L(L+1)\varepsilon_2^2\beta-\beta\varepsilon_2^3(n+s)]A_n(k_t)^{n+s}(r)^{n+s+1}\\&+\sum_{n=0}[k_t^2\varepsilon_2^3-3\beta^2\varepsilon_2(n+s)(n+s-1)-\beta^2\varepsilon_2(n+s)\\&-(3L^2+3L+1)\beta^2\varepsilon_2]A_n(k_t)^{n+s}(r)^{n+s+2}\\&+\sum_{n=0}[2\beta^3(n+s)^2+\beta^3(L^2+L-2)]A_n(k_t)^{n+s}(r)^{n+s+3}\\&-\sum_{n=0}[3k_t^2\varepsilon_2\beta^2]A_n(k_t)^{n+s}(r)^{n+s+4}\\&+\sum_{n=0}[2k_t^2\beta^3]A_n(k_t)^{n+s}(r)^{n+s+5}=0.\end{aligned} \tag{15}$$

Since by definition, A_0 can not be equal to zero, we can solve the first term for s, giving solutions $s=-1$ and 2. Since the region of interest includes the origin, the $s=-1$ solution is not valid, and $s=2$ is the only possible solution.

Constant anisotropy region

The solution in regions of constant anisotropy has been previously determined [17]. The radial solution is given solely in terms of Bessel functions of nonintegral order,

$$r^e\Pi^{(2)}=-\frac{1}{k_3^2}\sum_{L=1}^{\infty} i^{L-1}\frac{2L+1}{L(L+1)}\left(\frac{\pi k_3 r}{2}\right)^{1/2}\{c_L J_w(k_3 r)+d_L J_{-w}(k_3 r)\}P_L^{(1)}(\cos\theta)\cos\phi, \tag{16a}$$

$$w=\left(\frac{L(L+1)\varepsilon_t}{\varepsilon_r}+\frac{1}{4}\right)^{1/2}. \tag{16b}$$

IV. SMALL PARTICLE APPROXIMATION

In the limit of small particles ($k_t R\ll 1$), the term a_1 dominates the expression for C_{sca}. The potentials inside and outside the droplet may be expanded in a power series in r, and only the leading term in $k_t R$ is kept. In the small particle limit, the angular distribution of the scattered light is the

same as that of Rayleigh scattering [24]. However, the Rayleigh approximation ignores all details of the internal droplet structure, and takes into account only the average dielectric tensor, yielding the same scattering amplitude for all models of the anisotropy.

Linear model

Keeping only the first-order terms, the incident and scattered potentials have the forms

$$r\Pi^{(i)}=\left(\frac{\pi k_3 r}{2}\right)^2 \sin\theta\cos\phi, \tag{17a}$$

$$r\Pi^{(s)}=a_1\left(\frac{\pi k_3 r}{2}\right)^{-1} \sin\theta\cos\phi. \tag{17b}$$

Solving Eq. (15) for the potential inside the droplet, and keeping only those terms that will be first order in $k_t r$ at the interface, gives

$$r\Pi^{(2)}=A_0 k_t^2\left[r^2-\frac{\beta}{\varepsilon_2}r^3+\frac{9}{5}\frac{\beta^2}{\varepsilon_2^2}r^4-\frac{11}{5}\frac{\beta^3}{\varepsilon_2^3}r^5+\frac{131}{35}\frac{\beta^4}{\varepsilon_2^4}r^6-\frac{27}{5}\frac{\beta^5}{\varepsilon_2^5}r^7\right]\sin\theta\cos\phi. \tag{18}$$

Using the boundary conditions that E_θ and H_θ be continuous at the boundary lets us solve for a_1:

$$a_1=\frac{1}{3}\frac{\varepsilon_3\xi-2\varepsilon_t\eta}{\varepsilon_3\xi+\varepsilon_t\eta}(k_3R)^3, \tag{19a}$$

$$\xi=2-3\frac{\beta}{\varepsilon_2}R+\frac{36}{5}\frac{\beta^2}{\varepsilon_2^2}R^2-\frac{55}{5}\frac{\beta^3}{\varepsilon_2^3}R^3+\frac{786}{35}\frac{\beta^4}{\varepsilon_2^4}R^4-\frac{189}{5}\frac{\beta^5}{\varepsilon_2^5}R^5, \tag{19b}$$

$$\eta=1-\frac{\beta}{\varepsilon_2}R+\frac{9}{5}\frac{\beta^2}{\varepsilon_2^2}R^2-\frac{11}{5}\frac{\beta^3}{\varepsilon_2^3}R^3+\frac{131}{35}\frac{\beta^4}{\varepsilon_2^4}R^4-\frac{27}{5}\frac{\beta^5}{\varepsilon_2^5}R^5. \tag{19c}$$

Linear defect model

In the linear defect model, the dielectric anisotropy increases linearly with increasing radius, while the bulk of the droplet has constant anisotropy. The potential in the linear defect region is given to first order by Eq. (15). The potential in the constant anisotropy region is given to first order by

$$r\Pi^{(2)}=[c(k_t r)^{-1/2+w}+d(k_t r)^{-1/2-w}]\sin\theta\cos\phi. \tag{20}$$

Using the boundary conditions on E_θ and H_θ gives

$$a_1=\frac{1}{3}\frac{[(1/2+q)\varepsilon_3-2\varepsilon_t][(1/2-q)\eta-\xi]-[(1/2-q)\varepsilon_3-2\varepsilon_t][(1/2+q)\eta-\xi]\left(\frac{R_0}{R}\right)^{2q}}{[(1/2+q)\varepsilon_3+\varepsilon_t][(1/2-q)\eta-\xi]-[(1/2-q)\varepsilon_3+\varepsilon_t][(1/2+q)\eta-\xi]\left(\frac{R_0}{R}\right)^{2q}}(k_3R)^3. \tag{21}$$

η and ξ are the same as defined in Eq. (19), with R_0 substituted for R. q is defined as

$$q=w(L=1)=\left(\frac{2\varepsilon_t}{\varepsilon_r}+\frac{1}{4}\right)^{1/2}. \tag{22}$$

Isotropic defect model

The isotropic defect model, which consists of a region with constant anisotropy surrounding a small isotropic defect, has been previously solved [17]. We simply report the results here to use for comparison to the other models. We will assume in the following calculations that the dielectric constant of the central defect is the same as that of the nematic in the isotropic phase, i.e., $\varepsilon_1=\varepsilon_2$. The scattering amplitude for the droplet in the isotropic defect model is given as

$$a_1=\frac{2}{3}\frac{[(s+1)\varepsilon_r+\varepsilon_2][s\varepsilon_r-\varepsilon_3]-[s\varepsilon_r-\varepsilon_2][(s+1)\varepsilon_r+\varepsilon_3]\left(\frac{R_0}{R}\right)^{2s+1}}{[(s+1)\varepsilon_r+\varepsilon_2][s\varepsilon_r+2\varepsilon_3]-[s\varepsilon_r-\varepsilon_2][(s+1)\varepsilon_r-2\varepsilon_3]\left(\frac{R_0}{R}\right)^{2s+1}}(k_3R)^3, \tag{23a}$$

$$s=\left(\frac{2\varepsilon_t}{\varepsilon_r}+\frac{1}{4}\right)^{1/2}-1/2. \tag{23b}$$

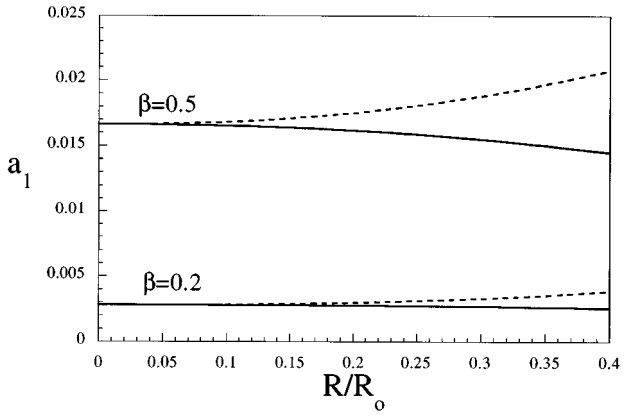

FIG. 2. Scattering amplitude as a function of defect size for the isotropic and linear defect models. The upper curve in each pair is from the linear defect model.

The small particle approximation is generally considered valid for $k_tR<0.2$. As k_tR becomes larger, terms that are higher order in k_tR become increasingly important. We have used the previous solution [17] for the isotropic defect model to calculate the first order correction to the scattering cross section. For the range of parameters used in Sec. V, we found the first-order correction to the cross section was less than 2.5% at $k_tR=0.5$, and was smaller for smaller values of k_tR. For larger values of k_tR, the contributions from other terms in Eq. (11) will become significant, and the complete sum must be evaluated.

V. NUMERICAL RESULTS

In this section we present numerical calculations of the scattering amplitudes for the various models of the anisotropy, and examine how the parameters of the model alter the magnitude of the scattering amplitude. In the following, the dielectric constant of the surrounding polymer is ε_3, the average dielectric constant of the nematic is ε_2, the anisotropy is β [see Eq. (12)], and the dielectric constant of the central defect region is ε_1.

A. Defect radius

Both the central and linear defect models contain a parameter, the size of the defect, R_0, that does not appear in the linear model. Previous studies [20,21] assumed a central defect that was up to 0.35 of the droplet radius. In Fig. 2 we present the dependence of the scattering amplitude on the defect radius for a system where the average dielectric constant of the nematic is the same as that of the polymer matrix ($\varepsilon_1=\varepsilon_2=\varepsilon_3=2$) for two distinct dielectric anisotropies (β). The positive curvature results are for the linear defect model, while those with negative curvature are for the isotropic defect model. The isotropic defect model shows little variation in the scattering amplitude up to $R/R_0=0.4$. The linear defect model, however, shows substantial variation at smaller values of the defect radius. The difference between these two models is solely due to the additional scattering introduced into the system by the changing dielectric constant in the defect region in the linear defect model. Unless otherwise specified, the following calculations will use $R_0/R=0.2$.

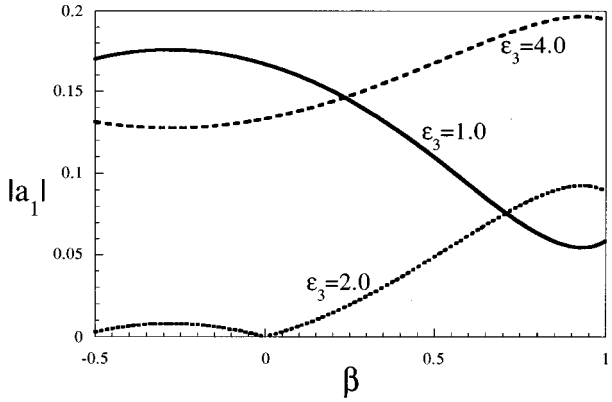

FIG. 3. Scattering amplitude vs anisotropy for the linear model.

B. Anisotropy dependence

In the linear model, the nematic dielectric susceptibility and anisotropy vary linearly with radius throughout the droplet. We show the relation between the scattering amplitude and the anisotropy in Fig. 3, with $\varepsilon_2=2.0$. We show the dependence on the anisotropy, β, for three distinct values ($\varepsilon_3=2.0$, 1.0, and 4.0) of the dielectric constant of the surrounding medium. The values of ε_3 were picked to match ε_2, and the values of ε_t and ε_r at maximum anisotropy, respectively. At small anisotropy, the scattering amplitude is much less when ε_3 is matched to ε_2. However, at large anisotropy there is a crossover, with smaller scattering occurring for $\varepsilon_3=1$. All three curves also exhibit an extremum, near $\beta=0.9$, with the $\varepsilon_3=1.0$ curve having a minimum. The general result is that scattering is smaller when ε_3 is matched to the average dielectric constant of the nematic. For negative anisotropy, the smallest scattering amplitude also occurs for $\varepsilon_3=2.0$, while the scattering from the other two values of ε_3 remains large across the whole negative anisotropy range.

The isotropic defect model differs from the linear model in assuming the nematic dielectric susceptibility and anisotropy is constant in the nematic region of the droplet. This is the model that has been used in previous scattering work [17–22]. We show the total scattering amplitude for the isotropic defect model in Fig. 4, again for $\varepsilon_3=2.0$, 1.0, and 4.0. In this model, the scattering amplitude is smallest when ε_3 is matched to ε_2, even at large anisotropy. At small anisotropy,

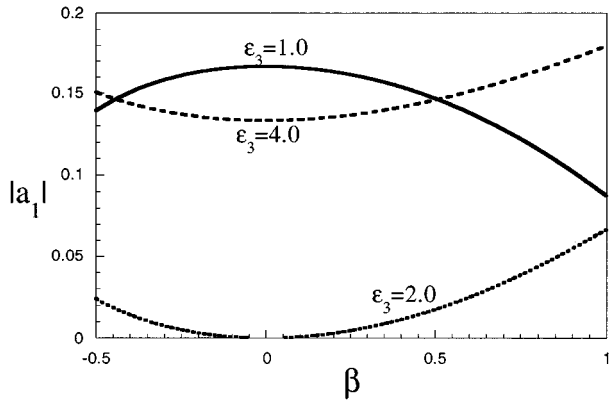

FIG. 4. Scattering amplitude vs anisotropy for the linear defect model. Results from the central defect model are similar.

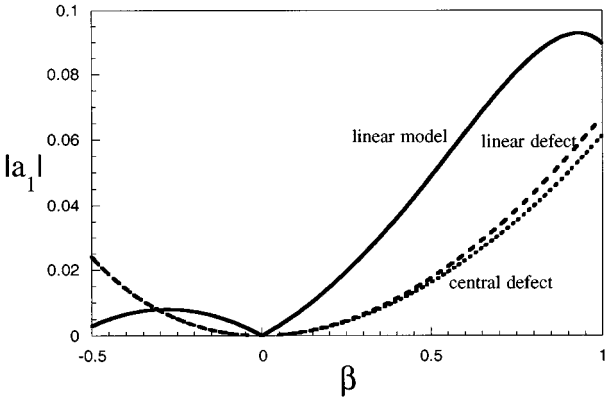

FIG. 5. Comparison of scattering amplitudes vs anisotropy for the three models.

the scattering amplitude for $\varepsilon_2=4.0$ is smaller than for $\varepsilon_2=1.0$, although, as the anisotropy increases, there is a crossover, with scattering smaller when $\varepsilon_3=1.0$. The results for the linear defect model are almost identical with those of the isotropic defect model, except for a slight increase in the curvature of the lines near $\beta=1$. The difference in the scattering amplitude is less than 8% between the two defect models.

Although the general behavior of the scattering amplitude as a function of the parameters of the nematic and polymer is qualitatively similar for the models, there are substantial quantitative differences between them. In Fig. 5, we show the scattering amplitude as a function of anisotropy for all three models with $\varepsilon_3=\varepsilon_2=2.0$. For positive anisotropy, the linear model has a much larger scattering amplitude than either of the defect models. At small positive anisotropy, the amplitudes differ by more than an order of magnitude. For negative anisotropies, the linear and defect models predict different behaviors with the linear model having a scattering maximum, while the defect models have scattering which increases with increasing negative anisotropy. As stated previously, there is little difference in the scattering amplitude for the linear defect and isotropic defect models.

The differences between the three models is shown more clearly in Fig. 6, which plots the ratio of the isotropic defect scattering amplitude to that of the linear defect model, and

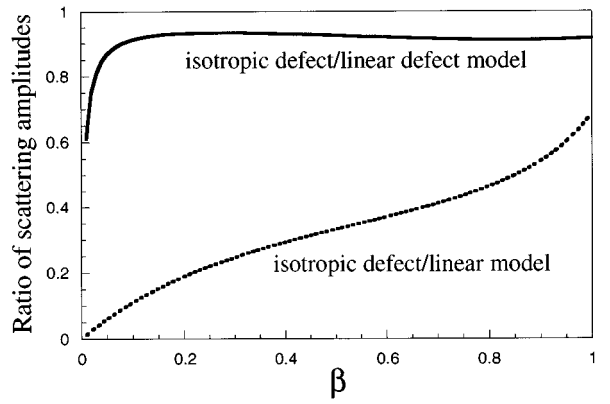

FIG. 6. Ratio of the scattering amplitude of the isotropic defect model to that of the linear model and ratio of the isotropic defect model to the linear defect model plotted as a function of anisotropy.

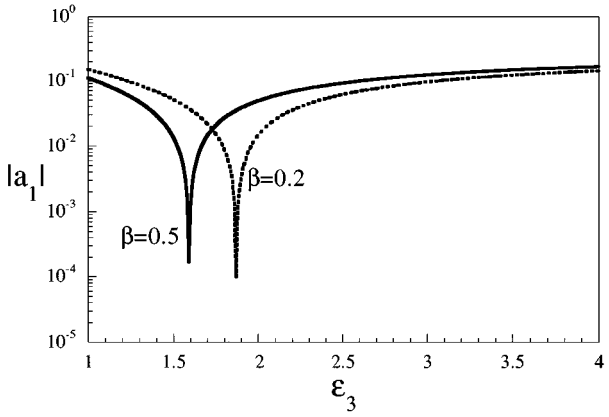

FIG. 7. Scattering amplitude as a function of the dielectric constant of the surrounding medium for the linear model.

that of the linear model. The ratios are shown only for positive anisotropies. The isotropic defect model, used in other work, gives scattering amplitudes smaller than those from the other models for the whole anisotropy range. For large anisotropy, the models all predict scattering of the same order of magnitude. However, for small anisotropy the scattering in the linear and linear defect models is qualitatively different from that of the isotropic defect model. Expansion of the scattering amplitude of the linear model [Eq. (19)] in the limit of small β gives a linear dependence on β, while the dependence of the isotropic defect model is of higher order. This is indicated by the rapid decrease in the ratio as the anisotropy approached zero. Because the scattering in the linear defect model is dominated by the defect scattering at small anisotropy, the scattering ratio between the isotropic defect and linear defect models also approaches zero as β approaches zero.

C. Dependence on the surrounding medium

The preceding calculations have shown that the scattering amplitudes are strongly dependent on the dielectric constant of the surrounding medium. This dependence is shown in more detail in Fig. 7, where we plot the logarithm of the scattering amplitude as a function of ε_3 for the linear model, with $\varepsilon_2=2.0$. The scattering is shown for two distinct values of the anisotropy. The scattering amplitude shows a strong dependence on the dielectric constant of the surrounding medium (ε_3), with the amplitude large across most of the range of ε_3. The place where the scattering amplitude goes to zero can be used to define the ''effective dielectric constant'' of the droplet. In the linear model, this effective dielectric constant is very close to the value of ε_t, which is equal to 2-β for this figure.

The results for both the linear and the linear defect models are similar, with one major difference. Both the defect models predict the minimum scattering point to occur for a value ε_3 of which is much closer to the value of the isotropic droplet than does the linear model. This is illustrated in Fig. 8, which compares the scattering as a function of ε_3 for the linear model and linear defect model, for an anisotropy of $\beta=0.2$. The minimum scattering point for the linear defect model occurs for a value of ε_3 which is slightly below that of the isotropic defect, while the minimum for the linear model

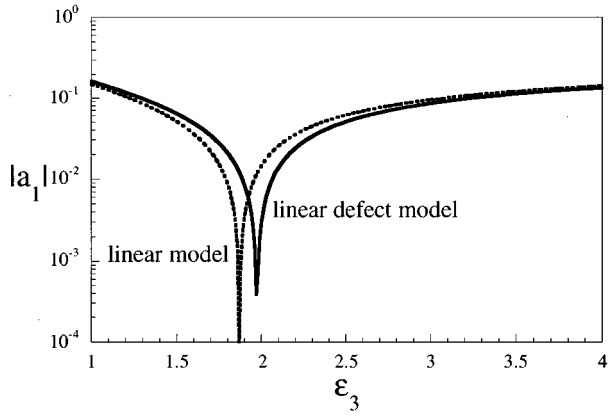

FIG. 8. Comparison of the scattering amplitude as a function of polymer dielectric constant for the linear and linear defect models.

occurs at a much smaller value of ε_3. This trend continues for all positive anisotropies. The results from the linear defect model are very similar to those from the isotropic defect model, with only a slight shift in the minimum scattering point toward larger value of ε_3 for the isotropic defect model.

We examine the condition for minimum scattering to occur in more detail in Fig. 9. Figure 9 plots the ''effective dielectric constant''of the droplet vs anisotropy for both the linear and linear defect models, with $\varepsilon_2=2.0$. The value of ε_t for all the values of anisotropy is also shown in the figure for reference. For positive anisotropy, the linear model predicts an effective dielectric constant for the droplet which is very close to the value of ε_t, except at very large anisotropy, while the linear defect model predicts an effective dielectric constant which is much closer to the isotropic value, which is $\varepsilon_2=2.0$. For negative anisotropy, the linear model still predicts an effective dielectric constant for the droplet which is between ε_t and the isotropic value for the droplet. The linear defect model, however, predicts that the effective dielectric constant for the droplet is still smaller than the dielectric constant of the isotropic droplet.

VI. DISCUSSION AND CONCLUSIONS

The development of PDLC devices has renewed interest in the scattering of light by small, radially anisotropic droplets. The droplets have the nematic director oriented along the radial axis of the droplet, due to the homeotropic anchoring of the nematic molecules at the droplet-polymer interface. Since the nematic molecules are optically anisotropic, the dielectric susceptibility inside the droplet has a radial anisotropy. Calculation of the scattering amplitude and cross section requires solution for the Debye potentials inside the droplet, which exhibit strong dependence on both the anisotropy of the nematic and the dielectric constant of the surrounding polymer. The dielectric anisotropy in the nematic is determined by the spatial variation of the order parameter, which is not known [23] analytically, but has been determined numerically elsewhere.

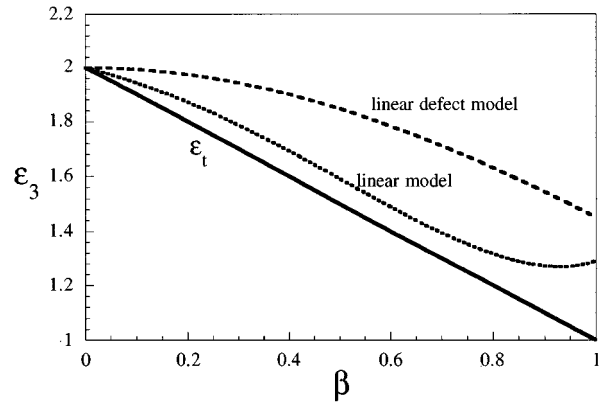

FIG. 9. Value of polymer dielectric constant to produce minimum scattering as a function of anisotropy for the linear model and linear defect model.

In this work, we have adopted three distinct models of the order parameter inside the droplet. The isotropic defect model, which assumes a small central isotropic defect surrounded by a region with constant order parameter (and constant dielectric anisotropy) has been used in previous scattering studies, and is particularly relevant for large ($R>0.22\ \mu$m) droplets. For small droplets ($R<0.22\ \mu$m) with strong anchoring, the order parameter can be represented by the linear defect model, which assumes a central defect in which the order parameter grows linearly, surrounded by a region of constant order parameter. For small droplets with weak surface anchoring, there is no simple model to describe the radial behavior of the order parameter, as there is no region of constant order parameter. To examine the significance of a constantly changing order dielectric anisotropy (order parameter) for scattering calculations, we have used the linear model, which assumes the order parameter increases linearly with radius.

We have derived the general form of the wave equation where the dielectric anisotropy is a function of r, and explicitly solved for the scattering amplitude of the three models in the small particle limit. The scattering amplitude in all three models depends on four parameters; the dielectric constant of the defect region ε_1, the dielectric constant of the surrounding polymer ε_3, the average dielectric constant of the nematic region ε_2, and the dielectric anisotropy β. For all the results shown, ε_1 was set equal to ε_2. In addition to these parameters, the two defect models have an additional parameter, R_0/R, which is the relative size of the defect. The size of the central defect, R_0/R, is not directly observable, but the results show that the scattering amplitude in the isotropic defect model is insensitive to the defect size for $R_0/R<0.4$. The scattering amplitude for the linear defect model shows larger variation in the scattering with defect size, with the scattering increasing as the defect radius increases.

Comparison of the scattering amplitudes calculated from the three models revealed some important qualitative as well as quantitative distinctions. The scattering amplitudes from the isotropic defect model were very similar to those from the linear defect model, using a reasonable value ($R_0/R=0.2$) for the defect radius. In the limit of small anisotropy, the linear model predicted much larger scattering amplitudes than either of the defect models. This is of importance in small droplets with weak anchoring, where the anisotropy is continuously varying throughout the droplet. The models also differ in predictions of the effective refractive index of the droplet, that is, the value of the dielectric constant of the

surrounding polymer which gives zero scattering. The linear model gives ''effective dielectric constants'' which are close to the value of the tangential component of the dielectric tensor in the nematic phase, while the defect models give an effective dielectric constant which is much closer to the isotropic value of the droplet.

In conclusion, we have shown the scattering amplitude of nematic droplets are complex functions of the nematic and polymer parameters. We have shown, in the small particle limit, that the scattering is strongly dependent on the variation of the dielectric anisotropy with radius in the droplet, and that the model with linear variation differs in many important respects from the standard model with an isotropic central defect and constant anisotropy. Quantitative determination of the scattering from droplets with radial anisotropy will require extension of these calculations to include both a more realistic model of the dielectric anisotropy, and solution when the droplet radius is approximately equal to the wavelength of the incident radiation.

ACKNOWLEDGMENTS

This work was supported by the U.S. Department of Energy, Office of Basic Energy Sciences under Contract No. DE-AC06-76RLO 1830. One of the authors (H.K.) received financial support from Abant Izzet Baysal University, Bolu, Turkey.

[1] J. W. Doane, Mater. Res. Bull. **16**, 22 (1991), and references therein.
[2] J. W. Doane, N. A. Vaz, B.-G. Wu, and S. Zumer, Appl. Phys. Lett. **48**, 4 (1986).
[3] J. Fergason, SID J. **16**, 68 (1985).
[4] A. Gollemme, S. Zumer, and J. W. Doane, Phys. Rev. A **37**, 559 (1988).
[5] Wei Huang and G. F. Tuthill, Phys. Rev. E **49**, 570 (1994).
[6] I. Vilfan, M. Vilfan, and S. Zumer, Phys. Rev. A **40**, 4724 (1989).
[7] J. Bajc and S. Zumer, Phys. Rev. E **55**, 2925 (1997).
[8] J. R. Kelly and P. Palffy-Muhoray, Mol. Cryst. Liq. Cryst. **243**, 11 (1994).
[9] J. B. Whitehead, S. Zumer, and J. W. Doane, J. Appl. Phys. **73**, 3 (1993).
[10] G. P. Crawford, A. Scharkowski, Y. K. Fung, J. W. Doane, and S. Zumer, Phys. Rev. E **52**, R1273 (1995).
[11] Z. Li and O. D. Lavrentovich, Phys. Rev. Lett. **73**, 979 (1994).
[12] J. H. Erdmann, S. Zumer, and J. W. Doane, Phys. Rev. Lett. **64**, 1907 (1990).
[13] P. Palffy-Muhoray, Michael A. Lee, and J. L. West, Mol. Cryst. Liq. Cryst. **179**, 445 (1990).
[14] G. E. Volovik and O. D. Lavrentovich, Zh. Eksp. Teor. Fiz. **85**, 1997 (1983) [Sov. Phys. JETP **58,** 1159 (1983)].
[15] S. Kralj and S. Zumer, Phys. Rev. A **45**, 2461 (1992).
[16] S. Chandresekhar, *Liquid Crystals*, 2nd ed. (Cambridge University Press, Cambridge, 1992).
[17] J. Roth and M. J. Dignam, J. Opt. Soc. Am. **63**, 308 (1973).
[18] S. R. Aragon and R. Pecora, J. Chem. Phys. **66**, 2506 (1977).
[19] B. Lange and S. R. Aragon, J. Chem. Phys. **92**, 4643 (1990).
[20] S. Zumer and J. W. Doane, Phys. Rev. A **34**, 3373 (1986).
[21] S. Zumer, Phys. Rev. A **37**, 4006 (1988).
[22] S. Zumer, J. Opt. Soc. Am. A **6**, 403 (1989).
[23] S. Kralj, S. Zumer, and D. W. Allender, Phys. Rev. A **43**, 2943 (1991).
[24] M. Kerker, *The Scattering of Light and Other Electromagnetic Radiation* (Academic, New York, 1969).
[25] *Electromagnetic and Acoustic Scattering By Simple Shapes*, edited by J. J. Bowman, T. B. A. Senior, and P. L. E. Uslenghi (North-Holland, Amsterdam, 1969).
[26] J. A. Stratton, *Electromagnetic Theory* (McGraw-Hill, New York, 1941).